

# Observation of Hubbard Bands in $\gamma$ -Manganese

S. Biermann\*,<sup>1</sup> A. Dallmeyer,<sup>1</sup> C. Carbone,<sup>1</sup> W. Eberhardt,<sup>1</sup> C. Pampuch,<sup>2</sup> O. Rader,<sup>2</sup> M. I. Katsnelson,<sup>3,4</sup> and A. I. Lichtenstein<sup>3</sup>

<sup>1</sup>*Institut für Festkörperforschung, Forschungszentrum Jülich, D-52425 Jülich, Germany*

<sup>2</sup>*BESSY, Albert-Einstein-Straße 15, D-12489 Berlin, Germany*

<sup>3</sup>*University of Nijmegen, NL-6525 ED Nijmegen, The Netherlands*

<sup>4</sup>*Institute of Metal Physics, 620219 Ekaterinburg, Russia*

(Dated: November 18, 2018)

We present angle-resolved photoemission spectra of the  $\gamma$ -phase of manganese as well as a theoretical analysis using a recently developed approach that combines density functional and dynamical mean field methods (LDA+DMFT). The comparison of experimental data and theoretical predictions allows us to identify effects of the Coulomb correlations, namely the presence of broad and undispersive Hubbard bands in this system.

PACS numbers: 71.20.Be, 79.60.-i, 71.15.Qe

The electronic theory of metals is based on the concept of quasiparticles, elementary excitations in the many-electron system that show a one-to-one correspondence with non-interacting electrons. They are characterized by a dispersion law describing the dependence of their energy on a quasimomentum, which can be measured by angle-resolved photoemission spectroscopy (ARPES) [1]. Hubbard showed for the first time, that strong electronic correlations can destroy this picture and result in the formation of so-called Hubbard bands of essentially many-body nature [2]. This concept is crucial for modern theories of strongly correlated electron systems [3]. The formation of Hubbard bands takes place, e.g., in many transition metal-oxide compounds, which thus have to be viewed as Mott insulators or doped Mott insulators [4]. Transition metals represent another class of systems where many-body effects are important (see [5] and Refs. therein). However, according to common belief, they are moderately correlated systems and normal Fermi liquids.

Electronic spectra of transition metals have been probed intensively by angle-resolved photoemission. Copper with its filled d-band was the first metal to be investigated thoroughly by this technique and the results were in excellent agreement with band structure calculations [6, 7]. The same technique, however, showed substantial deviations when applied to Ni and provided evidence for many-body behavior, such as the famous 6 eV satellite [8, 9]. The quasiparticle damping in iron can be as large as 30 % of the binding energy [10, 11]. Correlation effects are indeed important for metals with partially filled 3d bands and should be taken into account for an adequate description of ARPES spectra. Nevertheless, the main part of the spectral density in Fe is related to usual quasiparticles, and the spectral weight of the satellite in Ni amounts to only 20 % [11].

Investigations of an extended Hubbard model show

that correlation effects are strongest for half-filled d-bands [12]. Normally the geometrical frustrations in crystals (such as in the fcc-lattice) further enhance electronic correlations [3] so that one of the best candidates among the transition metals for the search of strong correlation effects is the fcc-( $\gamma$ ) phase of manganese. It is an example of a very strongly frustrated magnetic system; according to band-structure calculations [13] the antiferromagnetic ground state of  $\gamma$ -Mn lies extremely close to the boundary of the non-magnetic phase. Moreover, an anomalously low value of the bulk modulus [14] might be considered as a first experimental hint of strong electronic correlations.

The physical properties of bulk  $\gamma$ -Mn are hardly accessible in the experiment, since the  $\gamma$ -phase is only stable at temperatures between 1368 K and 1406 K, where it shows paramagnetic behavior. Thin films of  $\gamma$ -Mn, however, can be stabilized by epitaxial growth on Cu<sub>3</sub>Au(100) [15], which has an interatomic spacing (2.65 Å) very close to the interatomic spacing of Mn-rich alloys (2.60 – 2.68 Å). Schirmer et al. have shown that Cu<sub>3</sub>Au(100) supports layer-by-layer growth at room temperature up to coverages of 20 monolayers (ML) [15]. A low-energy electron diffraction (LEED) I(V) analysis revealed that the Mn films adopt the in-plane spacing of the Cu<sub>3</sub>Au(100) substrate and a comparatively large tetragonal distortion of the fcc-lattice. For the inner layers of a 16 ML Mn film, this distortion amounts to -6%, whereas the surface-subsurface distance is very close to the Cu<sub>3</sub>Au value.

We have used angle-resolved photoemission on the undulator beamline TGM-5 and on the TGM-1 beamline at BESSY to probe the electronic states in  $\gamma$ -Mn. The Cu<sub>3</sub>Au(100) substrate was prepared by repeated cycles of Ne<sup>+</sup> sputtering and annealing, until a very good LEED pattern with sharp diffraction spots and a low back-

ground intensity confirmed a high degree of structural order. The base pressure of  $2 \times 10^{-10}$  mbar rose to  $7 \times 10^{-10}$  mbar as Mn was deposited by electron beam evaporation. To avoid interdiffusion of Cu and Au, the onset of which was determined to be above room temperature [15] we used to keep the sample at room temperature during the Mn deposition and the photoemission measurements. The high quality of our Mn samples was routinely verified by means of LEED and Auger spectroscopy.

Angle-resolved photoemission measures the electron spectral density  $A(\mathbf{k}, E)$  as a function of the quasimomentum  $\mathbf{k}$  and the energy  $E$  multiplied by the Fermi distribution function  $f(E)$  [1]. For a given electron emission angle corresponding to a given  $\mathbf{k}$  the spectral density usually has a well-defined maximum as a function of  $E$  that determines the quasiparticle dispersion  $E(\mathbf{k})$  for the occupied part of the electronic bands. The experimental data (Fig. 1a) obtained for  $\gamma$ -Mn at a photon energy of 34 eV and for different electron emission angles, however, are characterized by two striking features. These are a weakly dispersive quasiparticle band near the Fermi level  $E_F$  and a broad and almost  $\mathbf{k}$ -independent maximum at approximately 2.5 eV below  $E_F$  [26]. These structures lack a significant dispersion also in spectra taken in normal electron emission for photon energies from 14 to 70 eV (Fig. 2). This behavior clearly distinguishes  $\gamma$ -Mn from other transition metals investigated with angle-resolved photoemission, which are strongly dispersive [16].

These data cannot be understood in the framework of a standard quasiparticle picture, since first-principles calculations of the band structure for different magnetic phases of  $\gamma$ -Mn show an energy dispersion of more than 1.5 eV [17]. Instead, the overall shape of the experimental spectra is very close to that of the Hubbard model on the metallic side of the Mott transition with a quasiparticle band near the Fermi level and a broad Hubbard band below  $E_F$  [18].

To test this hypothesis we have carried out first-principle (LDA+DMFT) calculations [19, 20] of the electronic structure of  $\gamma$ -Mn that include correlation effects in a local but fully dynamical approximation for the electron self-energy. In this approach a realistic description of the delocalized s and p electrons within the local density approximation (LDA) is supplemented by a term describing the partially localized nature of the d-states. The Hamiltonian thus reads

$$H = H^{LDA} + \frac{1}{2} \sum_{im'm'\sigma} U_{mm'}^i n_{im\sigma} n_{im'\sigma} + \frac{1}{2} \sum_{im \neq m' \sigma} (U_{mm'}^i - J_{mm'}^i) n_{im\sigma} n_{im'\sigma}, \quad (1)$$

where  $a_{im\sigma}^+$  [ $a_{im\sigma}$ ] creates [destroys] an electron with spin  $\sigma$  in state  $m$  at site  $i$  and  $n_{im\sigma} = a_{im\sigma}^+ a_{im\sigma}$  is the corresponding number operator.  $U_{mm'}$  and  $J_{mm'}$  are the

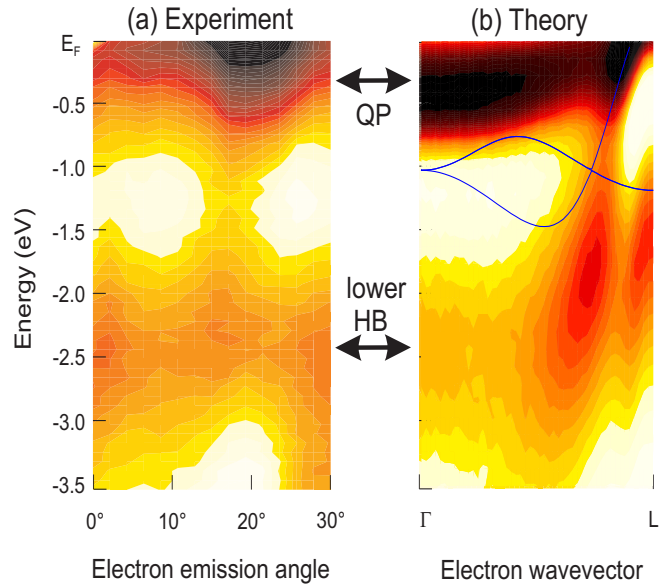


FIG. 1: Experimental photoemission spectra taken at a photon energy of 34 eV for different electron emission angles (a) in comparison with the spectral function  $A(\mathbf{k}, \omega)$  of  $\gamma$ -Mn as calculated within the LDA+DMFT approach (b). The  $\mathbf{k}$ -values corresponding to the experimental data vary approximately between the  $\Gamma$  and the  $L$  point in the Brillouin zone, binding energies are measured with respect to the Fermi energy. Colors from white, yellow, orange, red, brown to black denote increasing intensities. The blue lines in (b) give the LDA band structure.

direct and exchange term of the screened Coulomb interaction:  $U_{mm'} = \langle mm' | V_{scr}(\mathbf{r} - \mathbf{r}') | mm' \rangle$  and  $J_{mm'} = \langle mm' | V_{scr}(\mathbf{r} - \mathbf{r}') | m'm \rangle$ , which can be expressed in terms of the average Coulomb and exchange interaction parameters  $U$  and  $J$ , the values of which are known ( $U \sim 3$  eV,  $J \sim 0.9$  eV) [27] [28]. We use an LDA-LMTO [21] effective Hamiltonian  $H^{LDA}$ , corrected for double counting of the Coulomb energy of the d states in the usual way [20]. In Eq.(1) the sums run over the 3d states only, whereas in the LDA Hamiltonian, 4s, 3d and 4p states are included. The Coulomb interaction term is treated within the dynamical mean-field theory (DMFT) approach, which is the most efficient local approach: it reduces an original many-body lattice problem to the solution of an effective quantum impurity model in a self-consistent electron bath [3]. This multiband impurity problem has been solved by a numerically exact quantum Monte Carlo scheme based on the algorithm of Hirsch and Fye [22]. Using 64 or 128 slices in imaginary time allows to reliably access temperatures down to  $T \sim 500$  K. This is still higher than in the experiment; however, test cal-

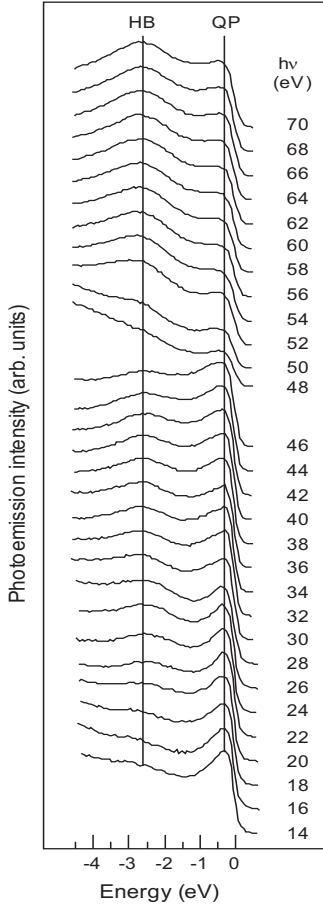


FIG. 2: ARPES spectra of a 17-monolayer  $\gamma$ -Mn film taken in normal emission at photon energies of 14 to 70 eV. The lack of dispersion distinguishes  $\gamma$ -Mn from other transition metals. Note that the spectral changes from 48 eV to 52 eV are due to resonant transitions between 3p and 3d states.

culations show that higher temperatures only result in a slight smoothening of the spectra, therefore justifying the comparison with the experimental data at lower temperature. Typically, about  $10^5$  QMC sweeps and 10 to 15 DMFT iterations are sufficient to reach convergence. The main quantities that we calculate and analyze are: a) the local Green's function, b) the  $k$ -resolved local Green's function

$$\hat{G}(\mathbf{k}, \tau) = \frac{1}{\beta} \sum_n e^{-i\omega_n \tau} \left( i\omega_n + \mu - \hat{H}^{LDA}(\mathbf{k}) - \hat{\Sigma}(i\omega) \right)^{-1} \quad (2)$$

where  $\omega_n$  are the Matsubara frequencies corresponding to the inverse temperature  $\beta$ . Inversion of the spectral representations of these functions by means of a Maximum Entropy scheme [23] yields the density of states (DOS)  $\rho(\omega)$  and the spectral function  $A(\mathbf{k}, \omega)$ . To our knowledge these calculations are the first ones that determine the  $\mathbf{k}$ -dependence of the spectral density for a

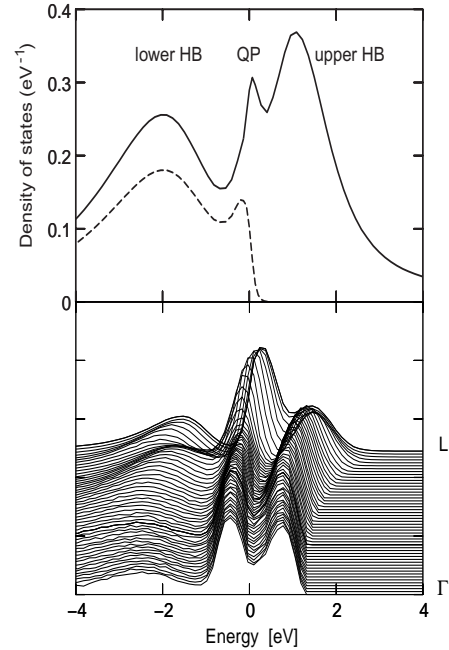


FIG. 3: Upper panel: density of states of  $\gamma$ -Mn as calculated within LDA+DMFT. The “three-peak structure” with the two broad Hubbard bands (HB) and a narrow quasiparticle (QP) Kondo resonance at the Fermi level (solid line) is typical of strongly correlated systems. The calculated photoemission spectrum (dashed line), i.e. the density of states multiplied with the Fermi function and broadened with the experimental resolution, shows reasonable agreement with the experimental spectra Fig. 1a and Fig. 2. Lower panel:  $\mathbf{k}$ -resolved density of states [arbitrary units] as calculated within LDA+DMFT. The different curves correspond to  $k$ -points between the  $\Gamma$  and the  $L$ -point.

material with  $d$ -states from LDA+DMFT with a realistic five-band Coulomb vertex.

The results are shown in Fig. 1b. For a given  $k$ -point there are two energy regions that carry the main part of the spectral weight: one narrow quasi-particle (QP) feature near the Fermi level and a very broad Hubbard band at about  $-2.5$  eV. Given the facts that (i) the experiments are done at a somewhat lower temperature than the calculations, that (ii) we do not take into account matrix elements for interpreting the photoemission data and that (iii) using the Maximum Entropy scheme for determining the spectral function, a quantity *not* directly measured within the Quantum Monte Carlo simulations, introduces a further approximation, the theoretical spectral function agrees reasonably well with the experimental data (Fig. 1a). Also plotted in Fig. 1b are the Kohn-Sham eigenvalues taken from the LDA calculation. The absence of LDA bands in the energy region carrying most of the spectral weight in this  $\mathbf{k}$ -space direction is strik-

ing and underlines the necessity of a proper many body treatment as done in LDA+DMFT. Note that assuming antiferromagnetic order (of the type detailed below) would slightly shift the LDA bands. However, the antiferromagnetic LDA band structure displays a dispersion of more than 2 eV and could thus not explain the undispersive photoemission feature.

The calculated ( $\mathbf{k}$ -integrated and  $\mathbf{k}$ -resolved) density of states curves (Fig. 3) demonstrate a characteristic "three-peak structure", with two broad Hubbard bands and a narrow quasiparticle Kondo resonance at the Fermi level which is typical of strongly correlated electron systems [3]. The quasiparticle peak at the Fermi level and the lower Hubbard band are seen in the present ARPES spectra; in  $\mathbf{k}$ -unresolved (BIS) measurements [24] a broad peak has been observed at 1.4 eV. To identify this peak with the upper Hubbard band (located at 1.2 eV in our calculations) one should prove the dispersionless nature of this peak. We have checked that all these incoherent features do not depend on the directions in  $\mathbf{k}$ -space used in our calculations. For the above reasons we believe that  $\gamma$ -Mn belongs to the class of strongly correlated materials and that the ARPES data can be considered as the first observation of Hubbard bands in a transition metal. As discussed above, correlation effects are indeed observed in other transition metals, e.g. the Ni satellite or some broadening of the quasi-particle bands in Fe. Still, even if the mechanism leading to these features is of the same origin, their spectral weight is not comparable to the weight of the Hubbard bands in  $\gamma$ -manganese.

The energy scale associated with the correlation effects that lead to the formation of the Hubbard bands ( $\sim U$ ) is much larger than that of the magnetic interactions. Therefore the observed effects are not very sensitive to long-range magnetic order. We have carried out the electronic structure calculations for both the paramagnetic and the antiferromagnetic structure with wave vector  $\mathbf{Q}=(\pi,0,0)$ , which is typical of  $\gamma$ -Mn-based alloys [25]. The magnetic ordering changes the electron spectrum little in comparison with the nonmagnetic case. However, in comparison with the results of standard band theory [13], the correlation effects stabilize the antiferromagnetic structure leading to a magnetic moment of about  $2.9 \mu_B$ .

According to the present results,  $\gamma$ -Mn can be considered a unique case of a strongly correlated transition metal. An even larger correlation would transform the system to a Mott insulator where every atomic multiplet forms its own narrow but dispersive Hubbard band [2, 4]. On the other hand, in most metals correlations are small enough for the quasiparticles to be well-defined in the whole energy region and usual band theory gives a reasonable description of the energy dispersion. Note that the correlation strength and bandwidth have almost the same magnitude for all 3d metals.  $\gamma$ -Mn is probably an exceptional case among the transition elements due to the half-filled d-band and geometric frustrations in the

fcc-structure.

In conclusion, our ARPES data for the  $\gamma$ -phase of manganese and their theoretical analysis by means of LDA+DMFT, an approach that accounts not only for band structure effects on the LDA level but also allows for a full description of local effects of strong Coulomb correlations, provide evidence for the formation of Hubbard bands in metallic manganese. This is a qualitatively new aspect in the physics of transition metals.

Acknowledgements: This research has been supported by a grant of supercomputing time at NIC Jülich and by Netherlands Organization for Scientific Research (NWO project 047-008-16).

\* Present address: LPS, CNRS-UMR 8502, UPS Bât. 510, 91405 Orsay, France

- [1] S. D. Kevan, *Angle-resolved photoemission: Theory and current applications*, vol. 74 (Elsevier, Amsterdam, 1992).
- [2] J. Hubbard, Proc. R. Soc. A **281**, 401 (1964).
- [3] For a review see A. Georges et al., Rev. Mod. Phys. **68**, 13 (1996).
- [4] N. F. Mott, *Metal-Insulator Transitions* (Taylor and Francis, London, 1974).
- [5] A. I. Lichtenstein, M. I. Katsnelson, and G. Kotliar, Phys. Rev. Lett. **87**, 067205 (2001).
- [6] P. Thiry et al., Phys. Rev. Lett. **43**, 82 (1979).
- [7] J. A. Knapp, F. J. Himpsel, and D. E. Eastman, Phys. Rev. B **19**, 4952 (1979).
- [8] S. Hüfner and G. K. Wertheim, Phys. Lett. A **51**, 299 (1975).
- [9] C. Guillot et al., Phys. Rev. Lett. **39**, 1632 (1977).
- [10] M. I. Katsnelson and A. I. Lichtenstein, J. Phys.: Condens. Matter **11**, 1037 (1999).
- [11] F. J. Himpsel, P. Heimann, and D. E. Eastman, J. Applied Phys. **52**, 1658 (1981).
- [12] N. E. Zein, Phys. Rev. B **52**, 11813 (1995).
- [13] V. L. Moruzzi, P. M. Marcus, and J. Kubler, Phys. Rev. B **39**, 6957 (1989).
- [14] A. F. Guillermet and G. Grimvall, Phys. Rev. B **40**, 1521 (1989).
- [15] B. Schirmer et al., Phys. Rev. B **60**, 5895 (1999).
- [16] O. Rader and W. Gudat, Landolt-Börnstein vol.III 23 C2 (Springer Verlag, Berlin, 1999).
- [17] D. J. Crockford, D. M. Bird, and M. W. Long, J. Phys.: Cond. Matt. **3**, 8665 (1991).
- [18] A. Georges and G. Kotliar, Phys. Rev. B **45**, 6479 (1992).
- [19] V. I. Anisimov et al., J. Phys.: Condens. Matter **9**, 7359 (1997).
- [20] A. I. Lichtenstein and M. I. Katsnelson, Phys. Rev. B **57**, 6884 (1998).
- [21] O. K. Andersen, Phys. Rev. B **12**, 3060 (1975).
- [22] J. E. Hirsch and R. M. Fye, Phys. Rev. Lett. **56**, 2521 (1986).
- [23] M. Jarrell and J. E. Gubernatis, Phys. Rep. **269**, 133 (1996).

- [24] W. Speier et al., Phys. Rev. B **30**, 6921 (1984).
- [25] R. S. Fishman and S. H. Liu, Phys. Rev. B **59**, 8681 (1999).
- [26] The 2.5 eV feature is insensitive to oxygen adsoption and therefore not related to surface-localized states.
- [27] We also performed calculations for other values of  $U$  (4 eV, 5 eV). Higher  $U$  values slightly shift the general features but do not lead to a qualitatively different behavior.
- [28] Moreover, we use the fact that for transition metals the ratio of the Slater integrals  $F_2/F_4$  is to a good approximation constant and equals 0.0625. Cf. V. I. Anisimov, F. Aryasetiawan, A. I. Lichtenstein, J. Phys.: Condens. Matter, **9** 767 (1997)